Three-dimensional Temporal Instability of Unsteady Pipe Flow

Avinash Nayak & Debopam Das
Dept. of Aerospace Engineering
Indian Institute of Technology Kanpur, India.
das@iitk.ac.in

Abstract: In this paper, 3-dimensional linear instability analysis has been carried out for unsteady pipe flow. An inflectional velocity profile from [2] has been considered and the stability analysis of it has been carried out for $n = 0$ (axisymmetric mode) and $n = 1 \& 2$. It was revealed that the profile is unstable for both axisymmetric and non-axisymmetric modes. The mode $n = 1$ was observed to be most unstable for this particular case considered. Both upstream and downstream moving disturbances have been observed as reverse flow exists in this flow. The vector plot of the disturbances showed the full shape and nature of the disturbances in the flow field. The predicted instability characteristics could explain the exact nature of visualized results of [2]. Wavelength of unstable disturbance from stability analysis and experimental observation of [2] matched well. The 3-D instability shows the observed helical nature of the flow.

1. Introduction:

Two types of unsteady viscous flow namely, zero and non-zero mean pulsatile flow and unsteady bluff body flow have received considerable attention in the literature. Pulsatile flow is important in the design of pumps and other process equipment. Blood flow in arteries and respiratory flow in trachea are also pulsatile in nature. Dynamic stall, related to unsteady boundary layer separation, is of importance in various aerodynamic applications including aircraft with high maneuverability, helicopter rotors, wind turbines, and jet engine compressor blades. A common feature in both these types of flows is the existence of inflection-point velocity profiles (often with reverse flow) that are unsteady [1-3].

Other than arterial hydrodynamics, pulsatile flow is also important in its application to MEMS microfluidic engineering applications. In many microfluidic devices that incorporate micro-scale pumping the flow is a pulsatile [4,5]. Flow pulsations provides a potential laminar mixing strategy for MEMS devices [6,7]. Our purpose in this paper is to understand the stability and transition to turbulence of such flows.

The oscillating flow may be generated by an oscillating piston in a pipe [1-2, 8-11]. In all cases the velocity profile is unsteady, often with reverse flow. In spite of the vast amount of literature a number of features regarding the stability and transition of such flows are not fully explained. In the experiments of Das & Arakeri [2] it was observed through flow visualization that unsteady velocity profiles with reverse flow in a pipe becomes unstable and forms series of vortices (see figure 1). The picture was taken illuminating a diametric plane with a light sheet. The vortices observed, appears to be a helical vortex in figure1. Ring vortices were also observed in some cases [2]. The exact explanation of the above phenomena is absent in literature. There is a need to solve the complete three-dimensional linear instability problem in cylindrical co-ordinate to understand the exact nature of the transition process.

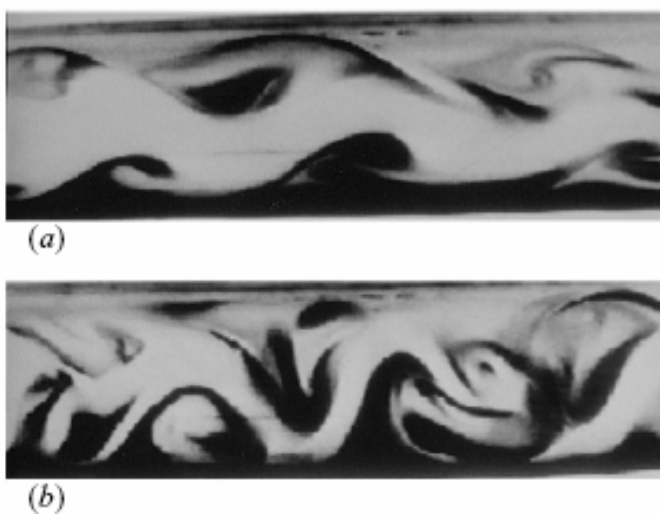

Figure 1. Flow visualization pictures showing development of azimuthal instability during deceleration stage of case II of [2]: (*a*) t = 9:88 s, t^*= 2:42, (*b*) t = 11:80 s, t^*= = 3:17.

There is no satisfactory linear stability analysis for time dependent flows in cylindrical co-ordinates with three-dimensional disturbances. Shen [12] has first carried out stability analysis for velocity profiles which are unsteady, but similar. Two common methods for stability analysis of unsteady flows have been the quasi-steady approximation and Floquet theory, which is only appropriate for periodic flows. The quasi-steady approximation explains observed instability in many unsteady situations [1-2, 13-15]. Direct numerical simulation [16] of oscillating pipe flow shows that infinitesimal disturbances evolve as would be predicted by quasi-steady stability analysis. Nonlinearity and secondary instability come into the picture only at later times and are essential to describe the final stages of transition.

2. Present problem:

In this paper complete three-dimensional linear instability analysis is carried out in cylindrical co-ordinate to understand and explain some of the phenomena observed in [1-2]. Considering axisymmetric parallel flow as the basic flow (solution is available in [1, 2 & 17]), perturbation equations can be obtained for Navier-Stokes equations and continuity equation. These four perturbation equations are linearized and further simplified assuming exponential dependence of the perturbation quantities on axial and angular space coordinates and on time as done in [18]. Temporal analysis of linear stability is done in many ways and is available in the literature. Four simultaneous equations are solved in [19] to obtain the eigenvalues. The power-series method and also the step by step contour integration method were used where as in [19] the matrix eigenvalue calculation for the linear stability of Hagen Poiseuille flow is carried out. The results in [19] are again corrected and presented in [20].

Among other methods available in the literature is discussed in [21], where all the velocity components can be eliminated to obtain a homogeneous equation in terms of pressure. As an alternative to the pressure formulation, the radial vorticity and the radial velocity can be used which results in two coupled equations. In [22] the stability analysis is done using the Sexl equation where the variables are changed to obtain two coupled ordinary differential equations of six degree.

In present work, the pressure and the axial component of velocity perturbation are eliminated to obtain two coupled equations with the highest degree as four for radial perturbation equation and

that of azimuthal component as three. Therefore, we derived total seven boundary conditions and solved for the eigenvalue using matrix method after discretising by finite difference technique. The results have been validated with the available literature data [20, 23 & 24] for the parabolic case and for both axisymmetric and non-axisymmetric modes. Further, using this method quasi-steady stability analysis is carried out for velocity profiles of different cases for flow, generated by trapezoidal piston motion [2].

3. Derivation of the Eigenvalue Problem:

The disturbance stream-function is assumed to be of the following form …

$$\{u, v, w, p\} = \{u(r), v(r), w(r), p(r)\}\exp[i\alpha(z-ct)+in\theta] \tag{1}$$

Both axisymmetric and non-axisymmetric mode of instability analysis is carried out with the quasi-steady assumption. As n is the node of the disturbance in the θ-direction, putting n=0 in the solution will give the formulation for the axisymmetric part. The disturbance quantities are substituted in perturbed Navier-Stokes equations in cylindrical coordinates and obtained are the governing equations for linear stability analysis as given in Eq.(1-5) [18] and [25].

1.Continuity:

$$u' + \frac{1}{r}u + i\left(\alpha w + \frac{n}{r}v\right) = 0 \tag{2}$$

2. r-momentum:

$$u'' + \frac{1}{r}u' - \left[\frac{1+n^2}{r^2} + \alpha^2 + i\alpha\,\mathrm{Re}(W-c)\right]u - \frac{2in}{r^2}v - \mathrm{Re}\,p' = 0 \tag{3}$$

3. θ-momentum:

$$v'' + \frac{1}{r}v' - \left[\frac{1+n^2}{r^2} + \alpha^2 + i\alpha\,\mathrm{Re}(W-c)\right]v + \frac{2in}{r^2}v - \frac{in}{r}\mathrm{Re}\,p = 0 \tag{4}$$

4. z-momentum:

$$w'' + \frac{1}{r}w' - \left[\frac{n^2}{r^2} + \alpha^2 + i\alpha\,\mathrm{Re}(W-c)\right]w - \mathrm{Re}\,vW' - re(i\alpha)p = 0 \tag{5}$$

Above ODE'S can be solved as an eigenvalue problem to obtain the linear instability characteristics of the velocity profiles.

From the continuity equation, the expression for w is obtained as:

$$w = \frac{i}{\alpha}\left[u' + \frac{1}{r}u + \frac{in}{r}v\right] \tag{6}$$

The above expression, Eq.8 can be used to determine w' and w'' in terms of u, v which can be substituted in the z-momentum equation to obtain the expression of pressure, p. With this expression, p and p' can be eliminated from the r and θ-momentum equations (Eq.3 and Eq.4 respectively). So that would give two coupled equations in u and v.

$$u'' + \frac{1}{r}u' - \left[\frac{1+n^2}{r^2} + \alpha + i\alpha\,\mathrm{Re}(W-c)\right]u - \frac{2in}{r^2}v$$
$$-\frac{1}{\alpha^2}\left[u^{iv} + \frac{2}{r}u''' - \frac{3}{r^2}u'' + \frac{3}{r^3}u' - \frac{3}{r^4}u\right]$$
$$-\frac{in}{\alpha^2}\left[\frac{1}{r}v''' - \frac{2}{r^2}v'' + \frac{3}{r^3}v' - \frac{3}{r^4}v\right]$$
$$+\left[\frac{n^2}{r^2} + \alpha^2 + i\alpha\,\mathrm{Re}(W-c)\right]\left\{\frac{1}{\alpha^2}\left[u'' + \frac{1}{r}u' - \frac{1}{r^2}u\right] + \frac{in}{\alpha^2}\left[\frac{1}{r}v' - \frac{1}{r^2}v\right]\right\} \quad (7)$$
$$+\left[-\frac{2n^2}{r^3} + i\alpha\,\mathrm{Re}\,W'\right]\left\{\frac{1}{\alpha^2}\left[u' + \frac{1}{r}u\right] + \frac{in}{\alpha^2}\left[\frac{1}{r}v\right]\right\}$$
$$-\frac{i}{\alpha}\mathrm{Re}\,u'W' - \frac{i}{\alpha}\mathrm{Re}\,uW'' = 0$$

$$v'' + \frac{1}{r}v' - \left[\frac{1+n^2}{r^2} + \alpha^2 + i\alpha\,\mathrm{Re}(W-c)\right]v + \frac{2in}{r^2}u$$
$$-\frac{in}{\alpha^2}\left[\frac{1}{r}u''' + \frac{2}{r^2}u'' - \frac{1}{r^3}u' + \frac{1}{r^4}u\right]$$
$$+\frac{n^2}{\alpha^2}\left[\frac{1}{r^2}v'' - \frac{1}{r^3}v' + \frac{1}{r^4}v\right] \quad (8)$$
$$+\frac{in}{r}\left[\frac{n^2}{r^2} + \alpha^2 + i\alpha\,\mathrm{Re}(W-c)\right]\left\{\frac{1}{\alpha^2}\left[u' + \frac{1}{r}u\right] + \frac{in}{\alpha^2}\left[\frac{1}{r}v\right]\right\}$$
$$+\frac{n}{\alpha}\mathrm{Re}\left(\frac{1}{r}u\right)W' = 0$$

The two equations are discretized using the central finite difference and it is written in the form $\left([A] - c[B]\right)\begin{Bmatrix} u \\ v \end{Bmatrix} = 0$. Then they are solved for the eigenvalues of c, for a particular value of α and Re, using MATLAB. This is for the temporal stability analysis of the problem and one can go ahead in the same manner for the spatial stability analysis also.

3.1. Boundary Conditions:

To obtain the solution, the boundary conditions should be properly determined. In these two sets of equations u has the highest 4th derivative while v has the highest 3rd derivative. Thus seven boundary conditions are required to solve these two coupled equations. Following are the boundary conditions given for different values of n.

n							
0	**R=0 (center-line)**	$u = 0$	$v = 0$	$u' = 0$			
	R=1 (at wall)	$u = 0$	$v = 0$	$u' = 0$			

1	**R=0 (center-line)**	$u+iv=0$		$u'=0$	$v'=0$	$\lim_{r\to 0} u \propto r^{n-1}$	
	R=1 (at wall)	$u=0$	$v=0$	$u'=0$			
2	**R=0 (center-line)**	$u=0$	$v=0$	$u'+iv'=0$		$3u''+2iv''=0$	
	R=1 (at wall)	$u=0$	$v=0$	$u'=0$			
>2	**R=0 (center-line)**	$u=0$	$v=0$	$u'=0$	$v'=0$		
	R=1 (at wall)	$u=0$	$v=0$	$u'=0$			

Table 1. Boundary conditions for perturbation velocities at wall and the centerline

a. For n=0, the two equations decouple to give a fourth order equation in u and a second order equation in v. So the boundary conditions given in the above table are enough.

b. For n=1, the available boundary conditions are not enough. One more condition will be required and it is given in the form $u \propto r^{n-1}$ when $\lim r \to 0$ [25]

4. Validation:

The results are obtained in the form of eigenvalues and eigenvectors for different α and different Reynolds number on temporal stability analysis. For the case of axisymmetric perturbation, the plot of imaginary part of eigenvalue versus the real part for $\alpha = 1$ and $\mathrm{Re} = 5000$ for pipe-parabolic flow is represented. This gives three distinct families of eigenvalues which exhibit a Y-shaped pattern in the (c_r, c_i)-plane. This can be directly compared with the results obtained in [23] using spectral method and also the results available of [24], where the asymptotic approach is followed.

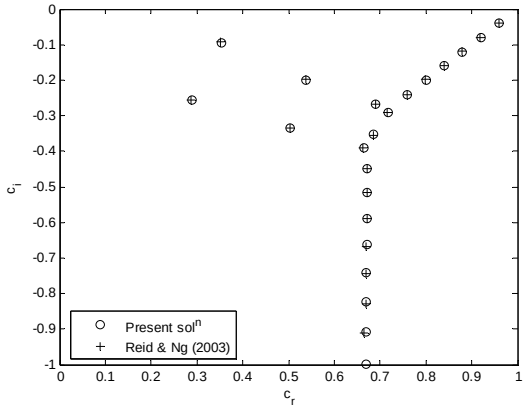

Fig.2 real vs imaginary part of eigenvalues for $\alpha = 1$ & $\mathrm{Re} = 5000$

In the report of [26], the less stable modes for $\alpha = 1$ and $\mathrm{Re} = 3000$ of pipe-parabolic flow for different n (azimuthal modes), i.e. both axisymmetric and non-axisymmetric cases have been presented. So, the eigenvalues for pipe parabolic flow for the same α and Reynolds number have

been calculated and have compared with the first few eigenvalues given in that paper. This validates our approach for the solution.

n	Meseguer & Trefethen (2003)		Our Solution	
	c_{real}	$c_{imaginary}$	c_{real}	$c_{imaginary}$
1	0.9114655676	-0.0412756446	0.9111601994	-0.0414589291
	0.3709350926	-0.0616190180	0.3709315590	-0.0616170543
	0.9582055429	-0.0883460251	0.9579140577	-0.0882260328
	0.8547888174	-0.0888701566	0.8544419785	-0.0890151521
2	0.8882976587	-0.0602856895	0.8853215894	-0.0617827903
	0.3525549270	-0.0878989803	0.3525437419	-0.0878832734
	0.8328933609	-0.1088383407	0.8297223598	-0.1096865226
	0.9394972195	-0.1120016161	0.9367328226	-0.1112532186
3	0.8643639210	-0.0832539769	0.8643760018	-0.0833083876
	0.3464019533	-0.1057084073	0.3463783096	-0.1056676461
	0.2149198697	-0.1168779213	0.2148760543	-0.1169101726
	0.8097468023	-0.1323924331	0.8098003259	-0.1325486670

Table. 2 Four most unstable eigenvalues for $\alpha = 1$ and $\mathrm{Re} = 3000$

5. Results and Discussions

In this section, an inflectional velocity profile is considered and the neutral stability curve is obtained for the same. The velocity profile considered here is one from the solutions obtained by Das & Arakeri (2000) for the flow created in a pipe by trapezoidal piston motion. After the piston has been stopped, the inflectional velocity profile is analyzed to obtain the range of α for a given Reynolds number for which the flow is unstable and the value of α for which the disturbance grows at the maximum rate. The aim is to predict the wave number and the growth-rate of disturbances that that will dominate the flow later on. Here, we have obtained the neutral stability curve for $n =$ 0, 1 and 2. For the larger n, the dissipation effect will be large enough to cause the flow be more stable for that mode. So, modes from higher n are not considered. In Fig.3 the plot of velocity profile is presented which has been used for the stability analysis. For this profile, the neutral stability curve has been obtained for $n =$ 0, 1, 2.

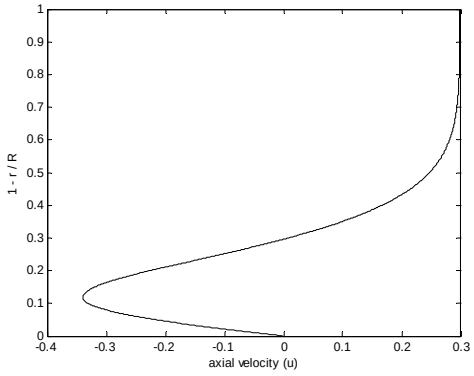

Fig. 3. Velocity Distribution that is used for stability analysis

For this flow, the parameter are given as follows (caseII of [2]: $t_0 = 0.42$, $t_1 = 3.68$, $t_2 = 4.04$, $t_p = 6.24$ $\mathrm{Re} = 2036.5$ & $U_p = 0.1591$ $0 - t_0$ is time for which piston accelerates linearly, $t_0 - t_1$ is time for which piston moves constantly $t_1 - t_2$ is time for which piston decelerates to

zero and t_p is time when a perceptible wave appears in pipe And the profile is obtained at $t = t_2 + \frac{1}{4}(t_p - t_2)$.

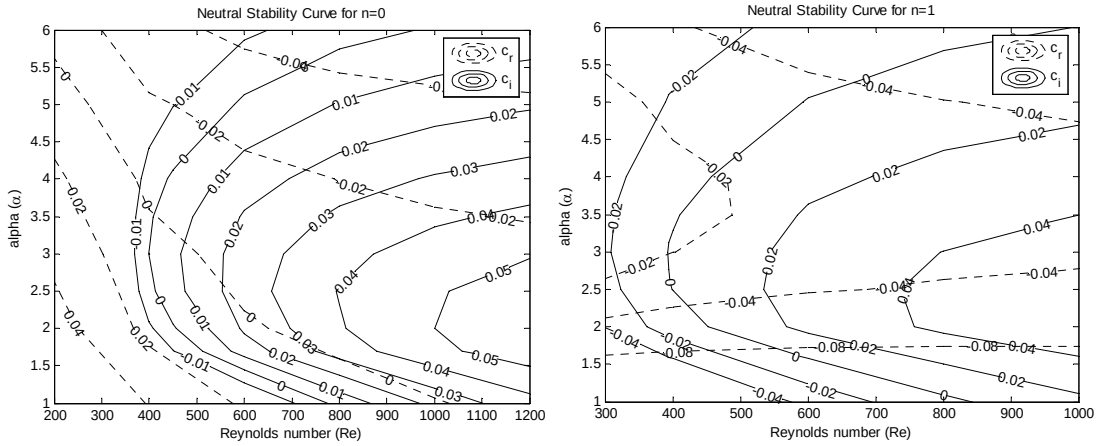

Fig. 4 Contour of real and imaginary part of the most unstable eigenvalue for n=0 and $n = 1$

In Fig.4 & 5 the contours for c_i and c_r for $n = 0,1 \& 2$ respectively are presented. Contours of c_i and c_r values shows that the critical Reynolds number for this curve is approximately 395 for $\alpha = 3$ and $n = 1$. Here, α is non-dimensionalized with respect to radius of the pipe. In fig 6 all three neutral curves are presented. We observe that n=1 mode is most unstable. This we expect that the nature of disturbance will be helical as seen in figure 1. For comparison with experimental result of Das & Arakeri (1998), α is rewritten as $\frac{\alpha}{\bar{\delta}}$, where $\bar{\delta}$ is the average boundary layer thickness over time t_1 to t. With this non-dimensionalization the value of $\frac{\lambda}{\bar{\delta}} \approx 3.22$. Thus it matches with the wavelength observed in experiment the value of which is approximately 3.0.

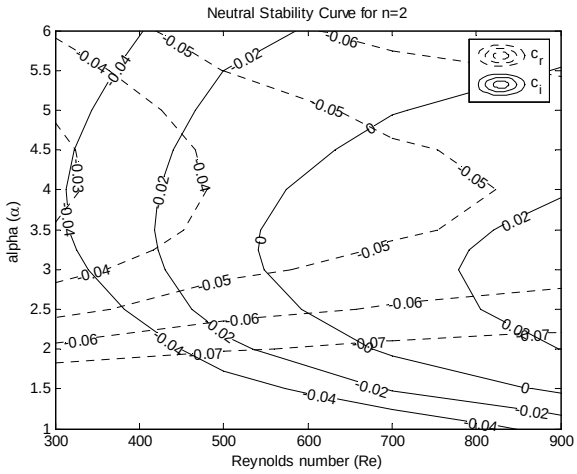

Fig. 5 Contour of real and imaginary part of the most unstable eigenvalue for $n = 2$

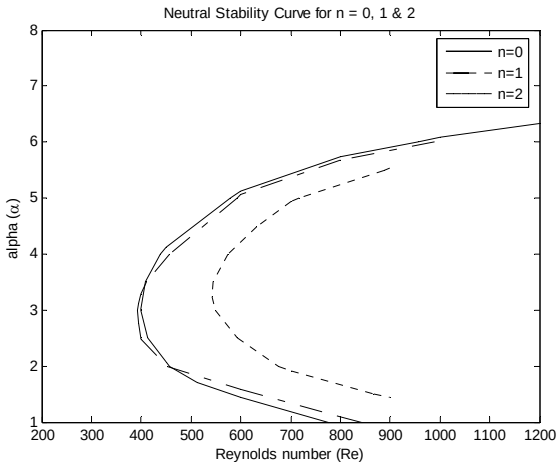

Fig. 6 Neutral Stability Curve for different n

The eigenvector plots of the most unstable mode are presented for $\alpha = 3$ and $\mathrm{Re} = 800$ and for both $n = 0$ and $n = 1$in fig 8 and 9. At a particular time the disturbances corresponding to the eigenvectors are also shown for $n = 0$ in fig 8. The vector plot is made in an axial and radial plane. For $n = 1$, Fig.9 shows the nature of disturbances in $r - \theta$ plane.

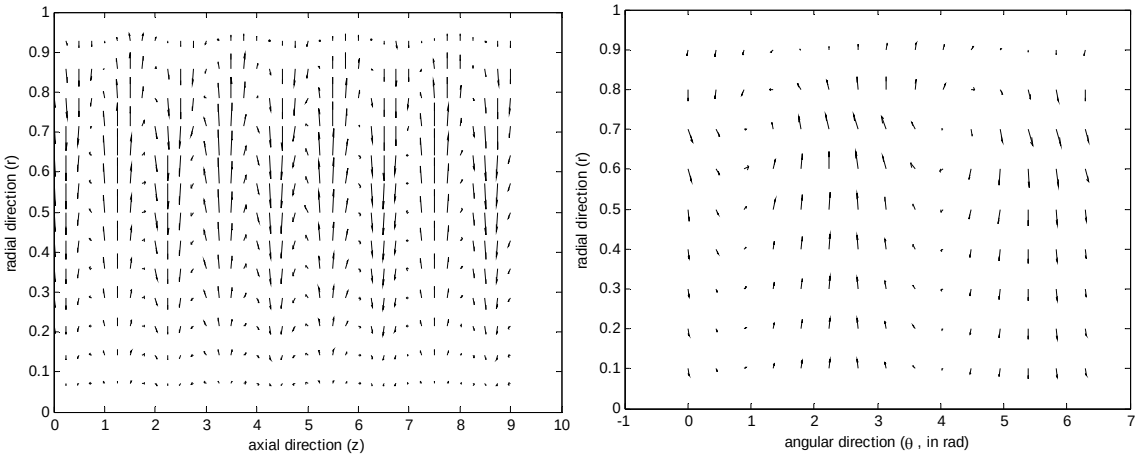

Fig. 7. (a) Distribution of disturbance in angular-radial plane for(a) $n = 1$, (b) n=0 for $\alpha = 3$ and $\mathrm{Re} = 800$.

6. Conclusion:

In this paper, 3-dimensional linear instability analysis has been carried out for unsteady pipe flow. The code has been validated for pipe parabolic flow by comparing with the data available in the literature. An inflectional velocity profile from [2] has been considered and the stability analysis of it has been carried out for $n = 0$ (axisymmetric mode) and $n = 1 \& 2$. It was revealed that the profile is unstable for both axisymmetric and non-axisymmetric modes. $n = 1$ was observed to be most unstable for this particular case considered. For some Reynolds number, the real part of the most unstable eigenvalue was coming out to be negative. That referred to the fact that the disturbances moving in negative direction can grow as reverse flow exists in this flow. The vector plot of the disturbances showed the full shape and nature of the disturbances in the flow field. The predicted wavelength of unstable disturbance from stability analysis and experimental observation of [2] matched well. The 3-D instability shows the observed helical nature of the flow.

7. References

1. Das, D. 1998 Evolution and instability of unsteady boundary-layers with reverse flow. Ph.D Thesis, Department of Mechanical Engineering, Indian Institute of Science, Bangalore.
2. Das, D. & Arakeri, J. H. 1998 Transition of unsteady velocity profiles with reverse flow. J. Fluid Mech. 374, 251-283.
3. Das, D. & Arakeri, J. H. 2000 Unsteady laminar duct flow with a given volume flow rate variation. Jl. Applied Mech. 67, 274-281.
4. [4] X. Geng, H. Yuan, H.N. Oguz, A. Prosperetti, Bubble-based micropump for electrically conducting liquids, J. Micromech. Microeng. 11 (2001) 270–276.
5. [5] K.P. Selverov, H.A. Stone, Peristaltically driven channel flows with applications toward micromixing, Phys. Fluids 13 (2001) 1837–1859.
6. [6] M. McGarry, D.L. Hitt, Numerical simulation of laminar mixing surfaces in converging microchannel flows, in: Computational Science & Its Applications-ICCSA 2003, in: Lecture Notes in Comput. Sci., vol. 26658, 2003, pp. 837–846.
7. [7] D.L. Hitt, M. McGarry, Numerical simulations of laminar mixing surfaces in pulsatile microchannel flows, J. Math. and Computers in Simul. (2003), in press.
8. Hino, M., Sawamoto, M. & Takasu, S. 1976 Experiments on transition to turbulence in an oscillating pipe flow. J. Fluid Mech. **75**, 193{207.
9. Akhavan, R., Kamm, R. D. & Shapiro, A. H. 1991*a* An investigation of transition to turbulence in bounded oscillatory Stokes flows. Part 1. Experiments. J. Fluid Mech. **225**, 395{422.
10. Ohmi, M., Iguchi, M., Kakehachi, K. & Masuda, T. 1982 Transition to turbulence and velocity distribution in an oscillating pipe flow. Bull. JSME **25**, 365{371.
11. Merkli, P. & Thomann, H. 1975 Transition to turbulence in oscillating pipe flow. J. Fluid Mech. **68**, 567{575.
12. Shen S. F. 1961 Some considerations on the laminar stability of time-dependent basic flows. J. Aero. Sci. **28**, 397{404 & 417).
13. Seminara, G. & Hall, P. 1975 Linear stability of slowly varying unsteady flows in a curved channel. Proc. R. Soc. Lond. A**346**, 279{303.
14. Hall, P. & Parker, K. H. 1976 The stability of the decaying flow in a suddenly blocked channel flow. J. Fluid. Mech. **75**, 305{314.
15. Obremski, H. J. & Fejer, A. A. 1967 Transition in oscillating boundary layer flows. J. Fluid Mech. **29**, 93{111.
16. Akhavan, R., Kamm, R. D. & Shapiro, A. H. 1991*b* An investigation of transition to turbulence in bounded oscillatory Stokes flows. Part 2. Numerical simulations. J. Fluid Mech. **225**, 423{444.
17. Nayak, A. 2005 M.Tech Thesis, Department of Aerospace Engineering, Indian Institute of Technology, Kanpur.
18. Lessen, M., Sadler, S. G. & Liu, T. Y. 1968 Stability of pipe poiseuille flow. Phys. Fluids. 11, 1404.
19. Salwen, H., Cotton, F. W. & Grosch, C. E. 1980 Linear stability of poiseuille flow in a circular pipe. J. fluid Mech. 98, 273-284.
20. Salwen, H. & Grosch, C. E. 1972 The stability of poiseuille flow in a pipe of circular cross-section. J. Fluid Mech. 54, 93-112.
21. Gustavsson, L. H. 1989 Direct resonance of nonaxisymmetric disturbances in pipe flow. Studies in Applied Mathematics. 80, 95-108.
22. Huang, L. M. & Chen, T. S. 1974 Stability of developing pipe flow subjected to non-axisymmetric disturbances. J. Fluid Mech. 63, 183-193.
23. Davey, A. & Drazin, P. G. 1969 The stability of poiseuille flow in a pipe. J. Fluid Mech. 36, 209-218.
24. Reid, W. H. & Ng, B. S. 2003 On the spectral problem for poiseuille flow in a circular pipe. Fluid Dynamics Research. 33, 5-16.
25. Batchelor, G. K. & Gill, A. E. 1962 Analysis of the stability of axisymmetric jets. J. Fluid Mech. 14, 529
26. Meseguer, A. & Trefethen, L. N. 2003 A spectral Petrov-Galerkin formulation for pipe flow I: linear stability and transient growth. Numerical Analysis Group Research Report. NA-00/18. Computing Laboratory, Oxford University.